Electronic Supplementary Material (ESI) for Nanoscale.
This journal is © The Royal Society of Chemistry 2023

Ultralow thermal conductivity of W-Janus Bilayers(WXY:X, Y=S, Se, Te) for thermoelectric devices

Neha Kapila Sharma[a]*,‡,Vivek Mahajan[a], Rajendra Adhikari[b], and Hitesh Sharma [a]*,‡
kapilaneha5@gmail.com; hitesh@ptu.ac.in

0.1 Supplementary Information Available

Table S 1 The lattice parameter(a), Binding energy(E_b) in eV, bond length, bond-angle (θ) and Energy Band-Gap (E_{Gap}) of WXY (XY= S, Se, Te) monolayers

System	a Å	WXY(XY= S, Se, Te) Å W-S,Se	Å W-Se,Te	θ ^{0}	E_b eV	E_{Gap} PBE eV
WSSe	3.25	2.43	2.54	81.70	-23.43	1.70
	3.24[1,2]	2.55[3]	2.43[3]			1.72[3]
WSeTe	3.44	2.57	2.74	82.64	-21.19	1.34
	3.44[4]	2.56[5]	2.72[5]			1.42[5]
WSTe	3.34	2.44	2.73	82.64	-21.33	1.26
	3.37[4]	2.45[3]	2.73[3]			1.23[3]

Table S 2 The lattice parameter(a), Binding energy(E_b) in eV, bond length(X-M-Y), bond-angle (θ) and Energy Band-Gap (E_{Gap}) of WSSe/WSTe HS

System	Stacking	S-W-Se Å	θ ^{0}	S-W-Te Å	θ ^{0}	E_b eV	E_{Gap} PBE eV
WSSe/WSTe (a=3.30Å)	AA	2.44,2.55	80.19	2.43,2.73	83.92	-1.34	0.27
	AA-I	2.43,2.55	80.12	2.42,2.72	83.89	-1.41	0.27
	AA-II	2.43,2.55	80.12	2.43,2.72	83.86	-1.39	0.25
	AB-I	2.44,2.55	80.15	2.43,2.72	83.86	-1.40	0.23
	AB-II	2.44,2.55	80.14	2.43,2.72	83.89	-1.43	0.24

Table S 3 The lattice parameter(a), Binding energy(E_b) in eV, bond length(X-M-Y), bond-angle (θ) and Energy Band-Gap (E_{Gap}) of WSeTe/WSTe HS

System	Stacking	Se-W-Te Å	θ ^{0}	S-W-Te Å	θ ^{0}	E_b eV	E_{Gap} PBE eV
WSeTe/WSTe (a=3.39Å)	AA	2.55,2.73	83.91	2.45,2.73	81.05	-1.42	0.59
	AA-I	2.55,2.73	83.85	2.45,2.73	80.97	-1.49	0.54
	AA-II	2.55,2.73	83.91	2.45,2.74	81.03	-1.43	0.58
	AB-I	2.55,2.73	83.87	2.45,2.73	80.93	-1.50	0.47
	AB-II	2.55,2.73	83.87	2.45,2.73	80.95	-1.49	0.52

Table S 4 The lattice parameter(a), Binding energy(E_b) in eV, bond length(X-M-Y), bond-angle (θ) and Energy Band-Gap (E_{Gap}) of WSSe/WSeTe HS

System	Stacking	S-W-Se Å	θ ^{0}	Se-W-Te Å	θ ^{0}	E_b eV	E_{Gap} PBE eV
WSSe/WSeTe (a=3.35Å)	AA	2.45,2.56	78.75	2.54,2.72	85.31	-1.26	0.11
	AA-I	2.44,2.56	78.75	2.54,2.72	85.27	-1.33	0.16
	AA-II	2.44,2.56	78.68	2.54,2.72	85.26	-1.35	0.20
	AB-I	2.45,2.56	78.67	2.55,2.72	85.27	-1.32	0.11
	AB-II	2.44,2.56	78.74	2.54,2.72	85.21	-1.33	0.09

[a] *Department of Physical Sciences, IKG Punjab Technical University, Kapurthala, Punjab, India*
[b] *Department of Physics,Kathmandu University,Nepal.*

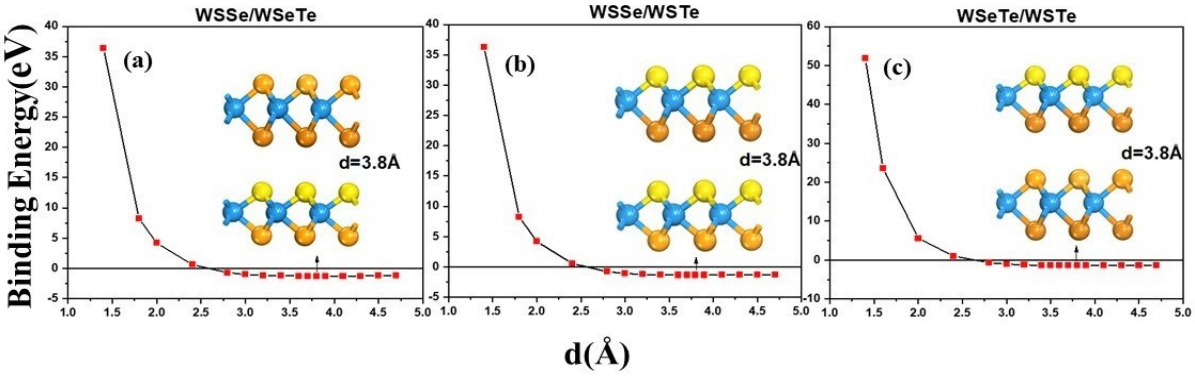

Figure S 1: Variation of binding energy with interlayer distance for (a)WSSe/WSTe HS, (b)WSeTe/WSTe HS, (c)WSSe/WSeTe HS.

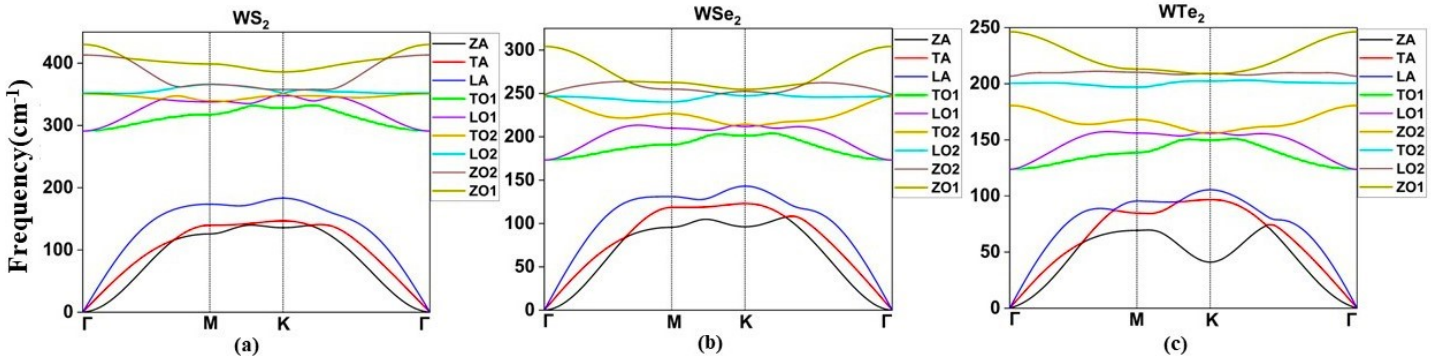

Figure S 2: Phonon Dispersion of (a) WS_2, (b) WSe_2, (c) WTe_2 monolayers. The term LA, TA and ZA are acoustic modes whereas LO-TO and ZOterms are optical modes. Both acoustic and optical modes start from Γ point and end at Γ point having no imaginary frequencies prediciting the thermal stability these layers.

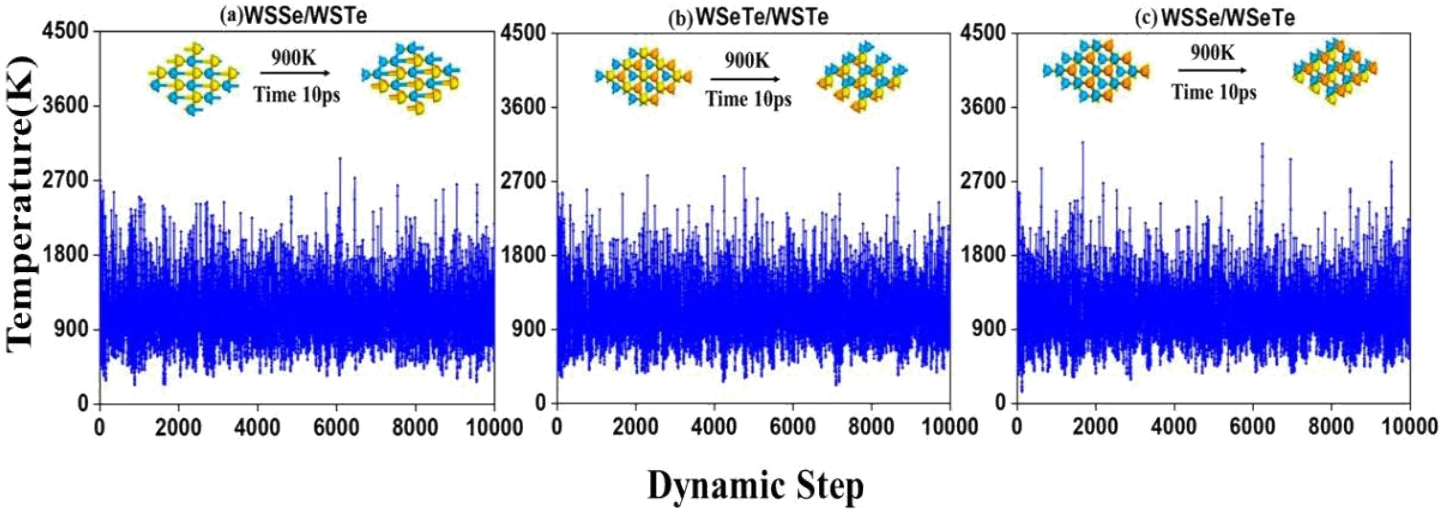

Figure S 3: Molecular dynamics simulations plot (a)WSSe/WSTe, (b)WSeTe/WSTe, and (c) WSSe/WSeTe HSs. The MD simulations have been performed using NVT ensemble average having a time step of 1femto seconds for 10,000(10ps) MD steps. The plot shows that all three HSs are dynamically stable at high temperatures as there is no bond-breaking or dislocation in the systems. Along with there is a snapshot of the system before and after heating in which the atoms revolve around their equilibrium position.

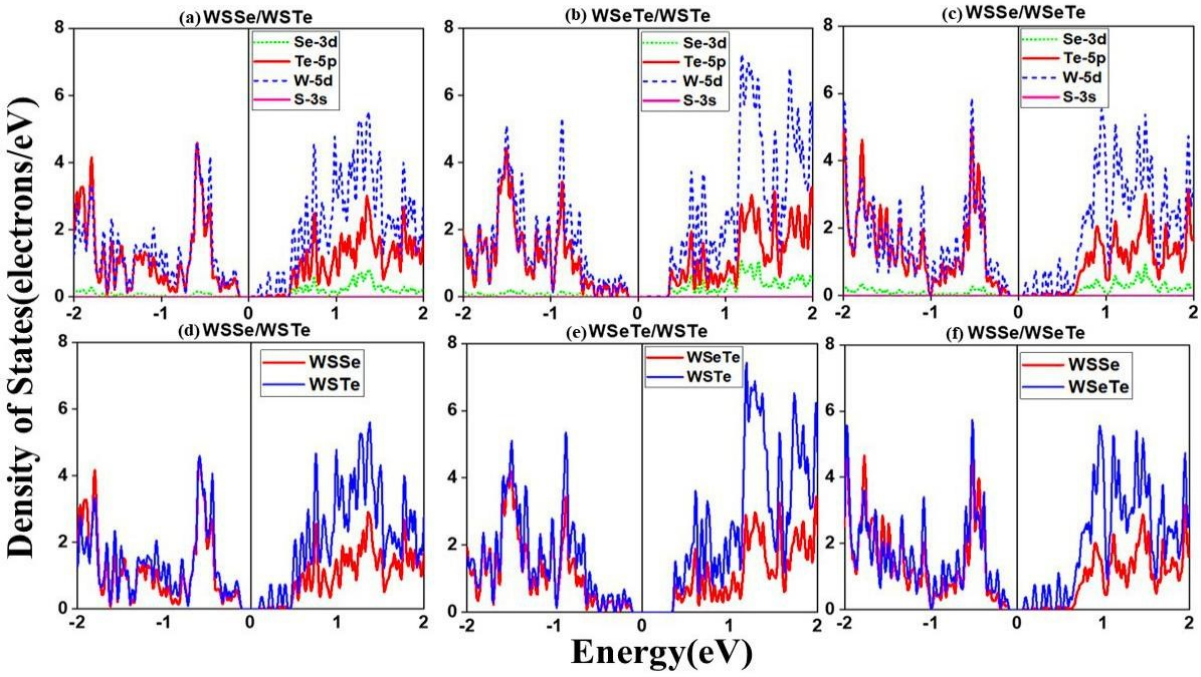

Figure S 4: Element-wise partial density of states (PDOS) plot for (a) WSSe/WSTe HS,(b) WSeTe/WSTe HS,(c) WSSe/WSeTe HS, and normal PDOS plots for (d) WSSe/WSTe HS,(e) WSeTe/WSTe HS,(f) WSSe/WSeTe HS predicting type II band alignment in all three HSs because of the CBM is filled with opposite layers first as that of VBM.

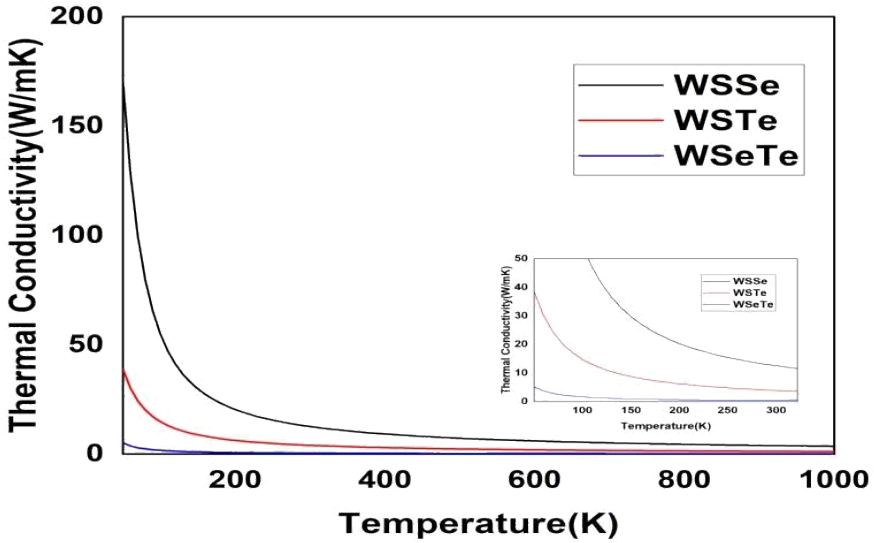

Figure S 5: Themal conductivity plot for WXY (XY =S, Se, Te) monolayers. Black color denoted WSSe , Red color denoted WSTe and Blue color denoted WSeTe.

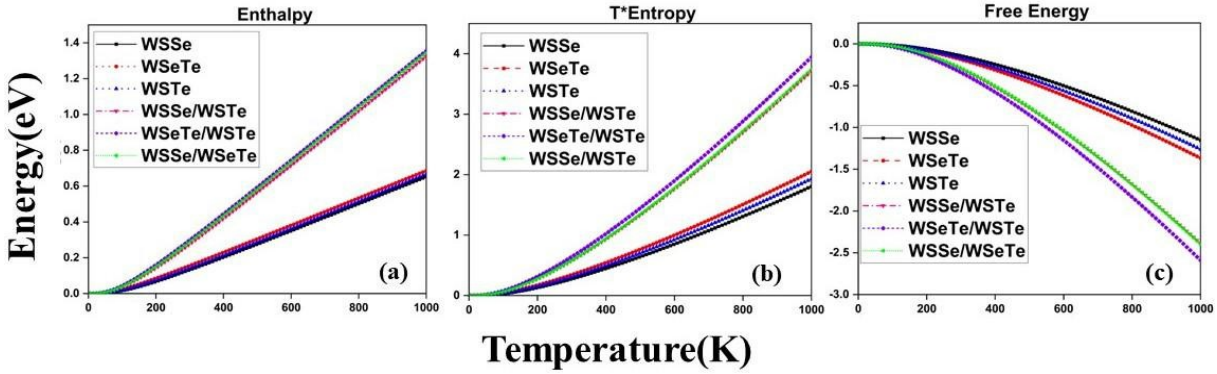

Figure S 6: (a) Enthalpy vs Temperature plot (b) Entropy vs Temperature plot, (c) Free Energy vs Temperature plot for WXY (XY= S, Se, Te) monolayers and their HSs. In all three plots, the monolayers are denoted by Black for WSSe, Red for WSeTe and Blue for WSTe whereas the HSs are denoted by Pink for WSSe/WSTe, Violet for WSeTe/WSTe, and Green for WSSe/WSeTe. In Figure S5(a),(b) the value of Enthalpy and Entropy is higher in HSs as compare to their monolayers whereas in Figure S5(c) the value of Free energy in HSs is lower as compared to their monolayers.

Notes and references

1 Y. C. Lin, C. Liu, Y. Yu, E. Zarkadoula E, M. Yoon M, A. A. Puretzky, L. Liang, Xi. Kong, Y. Gu, A. Strasser, M. H. Meyer, M. Lorenz, F. M. Chisholm, N. I. Ivanov, M. C. Rouleau, G. Duscher, K. Xiao, and B. D. Geohegan, Low Energy Implantation into Transition-Metal Dichalcogenide Monolayers to Form Janus Structures, ACS Nano 2020, 14, 4, 3896–3906, DOI:10.1021/acsnano.9b10196.

2 A. Kandemir, and H. Sahin, Bilayers of Janus WSSe: monitoring the stacking type via the vibrational spectrum, Phys. Chem. Chem. Phys., 2018,20, 17380-17386, DOI: 10.1039/C8CP02802H.

3 A. Patel, D. Singh, Y. Sonvane, P. B. Thakor, and R. Ahuja, High thermoelectric performance in two dimensional Janus monolayer material WS-X (X=Se, Te), ACS Appl. Mater. Interfaces 2020, 12, 41, 46212–46219, DOI: 10.1021/acsami.0c13960.

4 C. Y. Cheng, Y. Z. Zhu, M. Tahir, and U. Schwingenschlögl, Spin-orbit–induced spin splittings in polar transition metal dichalcogenide monolayers, EPL,2013, 102, 570-01, DOI: 10.1209/0295-5075/102/57001.

5 V. Vu. Tuan, V. H. Nguyen, V. P. Huynh, N. H. Nguyen, H. D. Bui M. Tdreesf, A. Bin, V. N. Chuong, Graphene/WSeTe van der Waals heterostructure: Controllable electronic properties and Schottky barrier via interlayer coupling and electric field, Applied Surface Science, 2020, 507, 145-036, DOI: 10.1016/j.apsusc.2019.145036